

Energy Efficient Federated Learning in Integrated Fog-Cloud Computing Enabled Internet-of-Things Networks

Mohammed S. Al-Abiad, *Student Member, IEEE*, Md. Zoheb Hassan, *Student Member, IEEE*, and Md. Jahangir Hossain, *Senior Member, IEEE*

Abstract—We investigate resource allocation scheme to reduce the energy consumption of federated learning (FL) in the integrated fog-cloud computing enabled Internet-of-things (IoT) networks. In the envisioned system, IoT devices are connected with the centralized cloud server (CS) via multiple fog access points (F-APs). We consider two different scenarios for training the local models. In the first scenario, local models are trained at the IoT devices and the F-APs upload the local model parameters to the CS. In the second scenario, local models are trained at the F-APs based on the collected data from the IoT devices and the F-APs collaborate with the CS for updating the model parameters. Our objective is to minimize the overall energy-consumption of both scenarios subject to FL time constraint. Towards this goal, we devise a joint optimization of scheduling of IoT devices with the F-APs, transmit power allocation, computation frequency allocation at the devices and F-APs and decouple it into two subproblems. In the first subproblem, we optimize the IoT device scheduling and power allocation, while in the second subproblem, we optimize the computation frequency allocation. For each scenario, we develop a conflict graph based solution to iteratively solve the two subproblems. Simulation results show that the proposed two schemes achieve a considerable performance gain in terms of the energy consumption minimization. The presented simulation results interestingly reveal that for a large number of IoT devices and large data sizes, it is more energy efficient to train the local models at the IoT devices instead of the F-APs.

Index Terms—Computation frequency control, energy consumption, federated learning, fog computing, Internet of Things (IoT), power control, quality of service (QoS).

I. INTRODUCTION

The emerging Internet-of-Things (IoT) leads to the unprecedented growth of the connected IoT devices in the wireless networks and significant rise of several computation demanding applications, such as interactive gaming, virtual/augmented reality, image/video processing. Cloud computing provides an efficient computation platform for executing the aforementioned applications. However, cloud computing requires efficient offloading of computation intensive tasks from the energy-constrained mobile devices to the cloud server (CS) of enormous computation capability [1]. In particular, the offloading of a task to a distant CS increases latency and security risk (e.g., important data should not be offloaded to CSs that are located outside a national territory) [2]. Hence, the benefit of cloud computing is diminished for the latency-sensitive and security critical applications [3]. Fog computing provides a complementary solution to the contemporary cloud

computing by reducing the distance between the computing CS and mobile devices [4].

In fog computing systems, fog access points (F-APs), with certain storage and computation capabilities, are deployed at the network edge [5]–[8]. As a result, mobile devices can offload the computation intensive tasks directly to the nearby F-APs instead of a distant CS, leading to the low-latency and fast access services. Moreover, an integration of fog and cloud computing provides a powerful computation and communication platform for the large number of IoT devices. Such an integrated architecture is referred as integrated fog-cloud computing (FCC)-enabled IoT system [9]. The integrated FCC provides powerful computation architecture for the IoT device, and it benefits from the centralized signal processing at the CS. Thereby, the integrated FCC can efficiently provide the required quality-of-service (QoS) for the emerging IoT applications.

Recently, the data driven decision making becomes an integral part of IoT networks, thanks to the availability of the enormous data and advancement of the devices' computing power. In particular, machine learning algorithms are extensively used to predict traffic congestion, user behavior, and QoS of users by analyzing large-scale data collected from the IoT devices. In conventional ML, the collected data from IoT devices (e.g., images, videos, and recorded audios) are offloaded to and processed in the centralized CSs, where the learning models are trained. Such a centralized ML approach is confronted by the huge traffic burden in the wireless links between IoT devices and core network. In addition, the privacy of users' sensitive data is impeded. Therefore, the conventional centralized learning method is inefficient for next generation IoT network [10]. Federated learning (FL) has been emerged as an efficient decentralized learning mechanism that allows multiple network edge devices to collaboratively learn a shared model [11]. In FL, the network edge devices train learning models locally based on local data. In contrast to the centralized learning mechanism, the devices only share updated model parameters with the CS. Subsequently, the CS calculates the global model parameter by aggregating local model updates from edge network. The local and global parameters are updated iteratively until convergence. By distributing the learning tasks between the network edge and centralized CSs, FL not only reduces the huge traffic burden over wireless channel, but also protects privacy of IoT data [12].

Due to the availability of distributed computing resources, an integrated FCC system provides a convenient platform to implement FL in wireless networks. In fact, using FL in integrated FCC system, the QoS of users can be sig-

Mohammed S. Al-Abiad and Md. Jahangir Hossain are with the School of Engineering, University of British Columbia, Kelowna, BC V1V 1V7, Canada (e-mail: m.saif@alumni.ubc.ca, jahangir.hossain@ubc.ca).

Md. Zoheb Hassan is with École de technologie supérieure (ETS), University of Quebec, Canada (e-mail: md-zoheb.hassan.1@ens.etsmtl.ca).

nificantly improved [13]. However, the channel impairments and interference present the key challenges to implement FL over wireless networks. Specifically, the FL training loss and convergence time jointly depends on selection of the collaborating devices, spectrum resource allocation, power allocation, and computation capability of the collaborating devices [14]. It is also imperative to reduce the energy consumption of the IoT devices participating in FL process. Particularly, IoT devices consume both communication and computation energy when the local models are trained at the IoT devices. To save the computation energy consumption, fog computing resources can be leveraged for local learning. However, in such a scenario, the communication energy consumption can be increased as the IoT devices need to upload a large amount of data to nearby F-APs with a strict latency constraint. To this end, we consider two different scenarios where the local models are trained either at the IoT devices or F-APs. For both scenarios, we develop resource allocation mechanisms to reduce energy consumption of FL with strict delay constraints.

A. Related Works and Motivations

Related works on communication-efficient FL: The performance of a decentralized ML depends on the optimization of wireless links between the network edge devices and parameter server (CS or fog computing nodes). Hence, it is imperative to optimally design the learning-centric resource allocation schemes [15]. In the recent literature, the design of communication-efficient FL was extensively studied. Leveraging the grouping of network edge devices and a decentralized group alternating direction method of multipliers, a jointly communication efficient and fast converging FL algorithm was proposed in [16]. To enhance the accuracy and convergence of FL, it is imperative to enhance the number of collaborating edge devices while using the available spectrum resources efficiently. To this end, a collaborative FL framework was proposed that allows resource constrained IoT devices to upload model parameters to the nearby devices instead of the distance CS [17]. Moreover, a joint scheduling of network edge devices and radio resource blocks (RRBs) was studied to minimize the FL loss function via applying Lyapunov optimization framework [18]. In a heterogeneous cellular network, a hierarchical FL framework can effectively enhance the number of devices participating in local learning [19]. In such a hierarchical FL framework, at each round, the network edge devices upload their model parameters only to the nearest F-APs (therein called small base-stations), and F-APs periodically upload the average local model parameters to the CS (therein called macro base-station) for a global aggregation. Thus, a large number of devices can participate in local learning. Besides, interference among the network edge devices can induce error in FL and increase the convergence time. Accordingly, interference aware radio resource allocation is also imperative for communication-efficient FL framework. A joint optimization of user selection, RRB allocation, and transmit power allocation was presented to minimize the loss function in FL training process. The authors in [20] proposed transmit power allocation of the IoT devices to enhance

information freshness in FL system. Considering the presence of eavesdroppers in an Internet-of-drones network, the authors in [21] proposed a secured and delay-constrained FL scheme through transmit power allocations.

Related works on energy-efficient FL: Since the mobile devices are battery-driven, for a sustainable operation of an FL framework, it is imperative to reduce energy consumption of the edge devices. In particular, an energy-efficient or green FL should consider minimizing communication and computation energy. In [22], energy-efficient radio resource allocation was proposed for delay constrained FL. However, the authors in [22] only minimized the communication energy and ignored the computation energy. In [23], the authors proposed an adaptive FL framework, where the devices can send quantized or compressed model parameters and thus, save energy. However, the radio resource optimization was not presented in [23]. In [24], radio resource allocation was developed to minimize both communication and computation energy in an FL system subject to delay constraints. However, the authors in [24] considered orthogonal multiple access (OMA) to connect edge devices with the base-station, which can limit the number of collaborating devices. Using OMA, the authors in [25] also proposed joint transmit power and computation frequency allocation to reduce overall energy consumption of FL in a fog-aided IoT network. The energy limitation of the collaborating edge devices can also be improved by energy-harvesting technique [26]. Moreover, the work in [27] considered a game theory framework to motivate the network edge devices to participate in local learning while reducing its energy consumption.

Motivations and Challenges: In contrast to the existing works [22]–[27], our motivation is to develop resource allocation mechanisms to facilitate energy-efficient FL in an integrated FCC-enabled IoT network. The considered architecture has a number of F-APs along with an CS, and the IoT devices are connected with the CS through F-APs. To improve the number of connected devices with F-APs using limited RRBs, an uplink non-OMA (NOMA) scheme [28] is considered. To the best of our knowledge, this is the first work that investigates efficient integration of joint cloud-fog computing and NOMA technique to reduce energy consumption of FL scheme. However, to take advantage of such an architecture for reducing energy consumption of FL, we need to develop a computationally efficient resource allocation scheme. Specifically, we need to address the following two challenges.

- **Challenge I:** In the first scenario, F-APs can work as relays where all the local learning is executed at the IoT devices. Alternatively, F-APs have the computation capability, and thus, they can participate in local learning along with the IoT devices. Therefore, in the second scenario, F-APs can work as local learning nodes to save the computation energy consumption of the connected IoT devices. Essentially, we need to investigate which of the aforementioned two scenarios has better energy-efficiency.
- **Challenge II:** There is an inherent trade-off between FL time and energy consumption. In particular, both computation and communication energy are increased

to reduce the FL time. Accordingly, to satisfy a given FL time constraint and reduce energy consumption, it is imperative to jointly optimize the degrees-of-freedom, namely, power allocation, IoT device scheduling to the F-APs/RRBs, and computation frequency allocation. However, an interplay of the aforementioned factors leads to a high computational complexity. Essentially, we need to develop a computationally efficient resource allocation scheme to address the trade-off between FL time and energy consumption.

B. Contributions

We investigate resource allocation for energy-efficient FL in an integrated FCC-enabled IoT network. Specifically, we propose a joint optimization of scheduling of IoT devices with the F-APs/RRBs, transmit power allocations, and computation frequency allocation at the IoT devices and F-APs. To this end, we introduce innovative graph-theoretical frameworks to develop computationally efficient solution. The main contributions of our work are as follows.

- 1) We consider two different scenarios for training the local model. In the first scenario, referred as *IoT device local learning*, local models are trained at the IoT devices and the F-APs upload the collected local model parameters to the CS for aggregation. In the second scenario, referred as *F-AP local learning*, the local models are trained at the F-APs based on the collected data from the IoT devices. For both scenarios, we aim at minimizing the overall energy consumption of IoT devices and F-APs subject to FL time constraint, IoT device-RRB/F-AP scheduling, transmit power allocations, and computation frequency allocation. Such a joint optimization problem is NP-hard and thus, computationally intractable. By analyzing the problem of each scenario, we decompose it into two subproblems namely, *resource scheduling and power allocation* subproblem and *computation frequency allocation* subproblem.
- 2) To solve the first subproblem, using graph theory, we design a low-complexity algorithm to optimize the scheduling among the IoT devices, F-APs, and RRBs. and transmit power levels of the IoT devices. In contrast, we obtain closed-form computation frequency allocation solution that depends on the scheduling obtained in the first subproblem. For both scenarios, efficient solutions are obtained by solving the aforementioned two subproblems alternately. The computational complexities of the proposed schemes are analyzed as well.
- 3) Extensive simulations are conducted to verify advantages of the proposed schemes over the benchmark schemes. Numerical results revealed that both proposed schemes offer improved energy consumption performances as compared to the benchmark schemes. The presented simulation results also interestingly reveal that for a large number of IoT devices and large data sizes, it is more energy efficient to train the local models at the IoT devices instead of the F-APs.

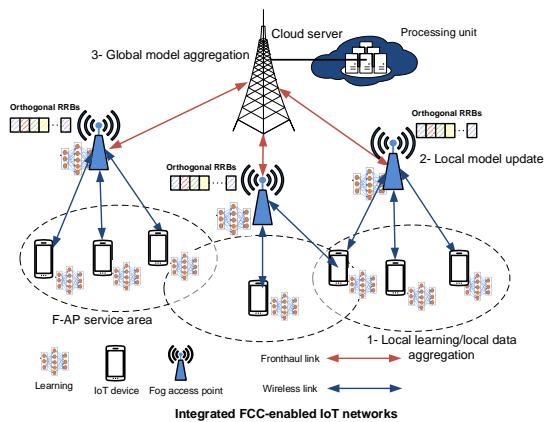


Fig. 1: Illustration of integrated FCC-enabled IoT networks

The rest of this paper is organized as follows. The system model is described in Section II. The optimization problems for the considered scenarios are provided in Section III. In Section IV and Section V, we develop two graph theory schemes to facilitate local learning at the IoT devices and F-APs, respectively. Simulation results are presented in Section VI, and in Section VII, we conclude the paper.

II. SYSTEM OVERVIEW

A. System Model

We consider an integrated FCC-enabled IoT system, illustrated in Fig. 1, that consists of one cloud server (CS), K F-APs, and N IoT devices. The sets of IoT devices and F-APs are denoted by $\mathcal{N} = \{1, 2, \dots, N\}$ and $\mathcal{K} = \{1, 2, \dots, K\}$, respectively. The N IoT devices (e.g., smartphones, laptops, and cameras) are connected to the F-APs which are connected to the CS using fronthaul links. We consider that each F-AP has a limited coverage range that represents the service area of the k -th F-AP within a circle of radius R . The set of IoT devices in the k -th F-AP's coverage range is defined by $\mathcal{N}_k = \{n \in \mathcal{N} | d_{k,n} \leq R\}$, where $d_{k,n}$ is the distance between the k -th F-AP and the n -th IoT device. Let $\mathbf{A} = a_{k,n}$ be the F-AP allocation matrix, where element $a_{k,n} = 1$ represents that the n -th IoT device is allocated to the k -th F-AP, and $a_{k,n} = 0$ otherwise.

Let \mathcal{D}_n denote the local data set of IoT device n , which is a set of data samples $\{x_i, y_i\}$, where x_i is sample i 's input (e.g., image pixels) and y_i is sample i 's output (e.g., label of the image). Similar to [23], [25], the local loss function on IoT device n 's data set can be calculated as $L_n(\omega) = \frac{1}{D_n} \sum_{i \in \mathcal{D}_n} l_i(\omega)$, $\forall n \in \mathcal{N}$, where $D_n = |\mathcal{D}_n|$ is the number of collected data samples by IoT device n and $l_i(\omega)$ is the loss function that measures the local training model error of data sample i . Then, IoT device n finds the optimum ω_n^* that minimizes $L_n(\omega)$ and uploads it to the suitable F-APs for aggregation by the CS. The IoT devices independently train local ML models based on their aggregated local data (e.g., images, videos, recorded audios). As shown in Fig. 1, the specific process of FL in the t -th iteration can be summarized as: 1) each IoT device downloads the global model parameters $\omega_n(t-1)$ from the CS through the nearest F-AP; 2) each IoT

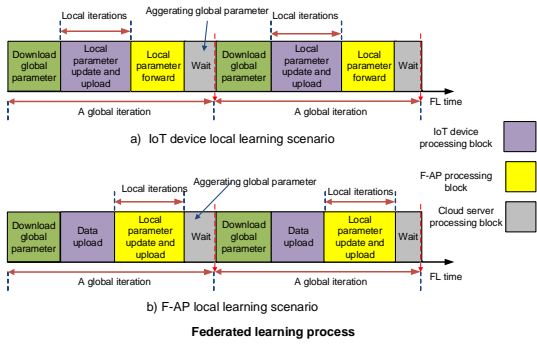


Fig. 2: Illustration of federated learning process.

device updates the local model by its local training data and sends the updated local model parameter $\omega_n(t)$ back to the F-APs; and 3) the CS aggregates the information from the F-APs and calculates the new global model parameters.

Each IoT device uploads the local information to the nearest F-AP via a wireless link. Similar to the resource setting in [29], [30], we consider that each F-AP has Z orthogonal RRBs that are denoted by the set $\mathcal{Z} = \{1, 2, \dots, Z\}$, where IoT devices can transmit their local information to the F-APs. These RRBs can be used practically as a generic term to denote time/frequency resource block of every F-AP, i.e., a group of orthogonal sub-carriers [5]. Let $\mathbf{S} = \{s_{k,z}^n\}$ be the RRB allocation matrix, where element $s_{k,z}^n = 1$ represents that the n -th IoT device is allocated to the k -th F-AP on the z -th RRB, and $s_{k,z}^n = 0$ otherwise. In this work, we consider a simple and efficient system's design where the scheduling-level coordination takes place, i.e., each user is only scheduled to a single RRB [5], [29], [30]. To schedule number of IoT devices to each RRB, we consider NOMA. Let p_n denote the transmission power of the n -th IoT device and let \mathbf{p} be a $1 \times N$ matrix containing the power levels of all IoT devices, i.e., $\mathbf{p} = [p_n]$. Hence, the instantaneous signal-to-interference-plus-noise (SINR) for the link between the n -th IoT device and the z -th RRB in the k -th F-AP is given by

$$\gamma_{k,z}^n = \frac{s_{k,z}^n p_n |G_{k,z}^n|^2}{\sum_{\substack{j \in \mathcal{N}_k \setminus n \\ G_{k,z}^j < G_{k,z}^n}} s_{k,z}^j p_j |G_{k,z}^j|^2 + \sigma^2}, \forall (j, n) \in \mathcal{N}_k, \quad (1)$$

where σ^2 denotes the additive white Gaussian noise variance and $G_{k,z}^n$ denotes the channel gain for the link between the n -th IoT device and the z -th RRB in the k -th F-AP. Then, the transmit rate of the n -th IoT device to the k -th F-AP over the z -th RRB can be given by $R_{k,z}^n = W \log_2(1 + \gamma_{k,z}^n)$, where W is the bandwidth of the z -th RRB. Consequently, the transmit rate of the n -th IoT device is $R_n = \sum_{k \in \mathcal{K}} \sum_{z \in \mathcal{Z}} W \log_2(1 + \gamma_{k,z}^n)$. At the F-APs, each F-AP uploads its collected local parameters to the CS through a fronthaul link of capacity R_{fh} .

In this work, we consider two different scenarios for training the local models: i) IoT device local learning and ii) F-AP local learning that are explained as follows.

B. IoT Device Local Learning Scenario

In this scenario, the role of IoT devices is to perform local training and upload the local parameters to the F-APs and

to the CS. The F-APs is only responsible for forwarding the collected local parameters from the IoT devices to the CS. This scenario is illustrated in Fig. 2-(a) and divided into FL time and energy consumption as follows.

1) *FL time*: In each iteration, the FL time consists of the computation time for local model training and the transmission time for uploading local model parameters to the F-APs as well as to the CS. In the local training process, IoT device n trains the local model and updates its local parameter until a local accuracy ϵ_l is achieved [23]. Let C_n denote the number of CPU cycles to process one data sample of IoT device n , and accordingly, the number of CPU cycles required for one local iteration over all data samples is $C_n D_n$. Therefore, the computation time for one local iteration in IoT device n can be calculated as $\frac{C_n D_n}{f_n}$, where f_n is the computational speed of the CPU in IoT device n (in cycles per second) [31]. Let \mathbf{f}_N be a $1 \times N$ matrix containing the computation frequency allocations of all IoT devices, i.e., $\mathbf{f}_N = [f_n]$. The number of local iterations to reach the local accuracy ϵ_l in IoT device n is $T_l = \frac{2}{(2-\delta\beta)\delta\vartheta} \ln(1/\epsilon_l)$, where δ, ϑ, β are constant parameters [21]. Then, the computation time of IoT device n is expressed as

$$T_n^c = T_l \frac{C_n D_n}{f_n}. \quad (2)$$

After performing the local learning at IoT device n , suppose that the data size d_n of each resulting local parameter ω_n is fixed over the learning process [32]. Hence, the transmission time of IoT device n for uploading its parameters to F-AP k on RRB z is $T_n^w = \frac{d_n}{R_{k,z}^n}$.

Note that the global model parameters can only be updated by the CS after all local model parameters are received from the F-APs. Consequently, the FL time τ_1 in each global iteration is determined by the longest duration time of receiving the parameters among all IoT devices and the longest duration time of forwarding the parameters from the F-APs to the CS. Moreover, the transmission duration of F-AP k to upload its collected parameters to the CS is $T_k^w = \frac{\sum_{n \in \mathcal{N}_k} d_n}{R_{fh}}$. Hence, the learning time τ_1 of one global iteration can be calculated as

$$\begin{aligned} \tau_1 &= \max_{n \in \mathcal{N}} \{T_n^c + T_n^w\} + \max_{k \in \mathcal{K}} \{T_k^w\} \\ &= \max_{n \in \mathcal{N}} \left\{ T_l \frac{C_n D_n}{f_n} + \frac{d_n}{R_{k,z}^n} \right\} + \max_{k \in \mathcal{K}} \left\{ \frac{\sum_{n \in \mathcal{N}_k} d_n}{R_{fh}} \right\}. \quad (3) \end{aligned}$$

The learning time τ_1 should satisfy the QoS requirement. Specifically, τ_1 should be no more than the maximum FL time T_q , i.e., $\tau_1 \leq T_q$. Hence, the QoS requirement can be expressed as

$$\max_{n \in \mathcal{N}} \left\{ T_l \frac{C_n D_n}{f_n} + \frac{d_n}{R_{k,z}^n} \right\} + \max_{k \in \mathcal{K}} \left\{ \frac{\sum_{n \in \mathcal{N}_k} d_n}{R_{fh}} \right\} \leq T_q, \quad (4)$$

and can be written as

$$T_l \frac{C_n D_n}{f_n} + \frac{d_n}{R_{k,z}^n} + \frac{\sum_{n \in \mathcal{N}_k} d_n}{R_{fh}} \leq T_q, \forall n \in \mathcal{N}, \forall k \in \mathcal{K}. \quad (5)$$

2) *Energy consumption model*: The IoT device's energy is consumed for both local model training and parameter transmission over wireless links that is explained as follows.

- *Local computation*: We adopt the widely used energy consumption model which considers that the energy con-

sumption of IoT device n to process a single CPU cycle is αf_n^2 , where α is a constant related to the switched capacitance [33], [34]. Hence, the energy consumption of IoT device n for local computation is $E_n^c = T_l C_n D_n \alpha f_n^2$ [21].

- *Parameter transmission:* The energy consumption to upload local model parameters to the F-APs over wireless links can be denoted by E_n^w and calculated as $p_n T_n^w$. Since the local parameters are forwarded from the F-APs to the CS over high transmission links, the energy consumption is negligible. Hence, we discard the F-APs' energy consumption.

By combining all the aforementioned terms of energy consumption, the total energy consumption of the system in the IoT device local learning scenario can be calculated as

$$E = \sum_{n \in \mathcal{N}} (E_n^w + E_n^c) = \sum_{n \in \mathcal{N}} \left[\frac{p_n d_n}{R_{k,z}^n} + T_l C_n D_n \alpha f_n^2 \right]. \quad (6)$$

C. F-AP Local Learning Scenario

The IoT devices, in this scenario, are solely responsible for uploading their data to the F-APs. The F-APs, then, train local models using these collected data and upload the resulting local parameters to the CS for global aggregation. This scenario is illustrated in Fig. 2-(b). The FL time and energy consumption of this scenario are explained as follows.

1) *FL time:* In each iteration, the FL time consists of the transmission time for uploading the data from IoT devices to F-APs, the computation time for training local models at the F-APs, and the transmission time for uploading the resulting local model parameters to the CS. Consider that the data size D_n of the uploaded data \mathcal{D}_n by IoT device $n \in \mathcal{N}_k$ is fixed over the learning process [32]. The transmission time for uploading data from IoT devices \mathcal{N}_k to F-AP k is written as

$$T_k^w = \max_{n \in \mathcal{N}_k} \left\{ \frac{D_n}{R_{k,z}^n} \right\}, \forall z \in \mathcal{Z}. \quad (7)$$

Each F-AP k iteratively trains the local learning model on the collected data and updates its local parameter $\omega_k(t)$ until a local accuracy ϵ_l is achieved. Let C_k denote the number of CPU cycles to process one data sample of F-AP k . Hence, the number of CPU cycles required for one local iteration is $C_k B_k$, where B_k is the number of uploaded data samples \mathcal{B}_k to F-AP k , i.e., $B_k = |\mathcal{B}_k|$ and $\mathcal{B}_k = \cup_{n \in \mathcal{N}_k} \mathcal{D}_n$. Therefore, the computation time for one local iteration at F-AP k can be calculated as $\frac{C_k B_k}{f_k}$, where f_k is the computational speed of the CPU in F-AP k (in cycles per second). Let \mathbf{f}_K be a $1 \times K$ matrix containing the computation frequency allocations of all F-APs, i.e., $\mathbf{f}_K = [f_k]$. Consider that the number of local iterations of F-APs to reach the local accuracy ϵ_l is T_l . Then, the computation time of F-AP k is expressed as

$$T_k^c = T_l \frac{C_k B_k}{f_k}. \quad (8)$$

Since the global model parameters can only be updated after all local model parameters are received from the F-APs, the FL time τ_2 in each global iteration is determined by the longest time for uploading data to F-APs, training local models at the F-APs, and the longest time for transmitting the parameters

from the F-APs to the CS. Thus, the learning time τ_2 of one global iteration can be calculated as

$$\begin{aligned} \tau_2 &= \max_{k \in \mathcal{K}} \{T_k^w + T_k^c + T_k\} \\ &= \max_{k \in \mathcal{K}} \left\{ \max_{n \in \mathcal{N}_k} \left\{ \frac{D_n}{R_{k,z}^n} \right\} + T_l \frac{C_k B_k}{f_k} + \frac{d_k}{R_{fh}} \right\}, \quad (9) \end{aligned}$$

where d_k is the local parameter size of F-AP k . Similar to the first scenario, the learning time τ_2 should satisfy the QoS requirement, i.e., $\tau_2 \leq T_q$. Thus, the QoS requirement can be expressed as

$$\max_{k \in \mathcal{K}} \left\{ \max_{n \in \mathcal{N}_k} \left\{ \frac{D_n}{R_{k,z}^n} \right\} + T_l \frac{C_k B_k}{f_k} + \frac{d_k}{R_{fh}} \right\} \leq T_q, \quad (10)$$

and can be written per F-AP as

$$\max_{n \in \mathcal{N}_k} \left\{ \frac{D_n}{R_{k,z}^n} \right\} + T_l \frac{C_k B_k}{f_k} + \frac{d_k}{R_{fh}} \leq T_q, \forall k \in \mathcal{K}. \quad (11)$$

2) *Energy consumption model:* The IoT device's energy is consumed for data transmission over wireless links, which is $E_n^w = p_n T_n^w = \frac{p_n D_n}{R_{k,z}^n}$. For the F-APs, the energy consumption is explained as follows.

- *Local computation:* The energy consumption model of F-AP k for processing a single CPU cycle is αf_k^2 . Thus, the energy consumption of F-AP k for local computation is expressed as $E_k^c = T_l C_k B_k \alpha f_k^2$ [21].
- *Parameter transmission:* The energy consumption for uploading local model parameters to the CS is $E_k^w = q_k T_k^w = \frac{q_k d_k}{R_{fh}}$, where q_k is the transmit power of F-AP k .

By combining all the aforementioned terms of energy consumption, the total energy consumption of all IoT devices and F-APs in the second scenario can be calculated as

$$\begin{aligned} E &= \sum_{n \in \mathcal{N}} E_n^w + \sum_{k \in \mathcal{K}} (E_k^w + E_k^c) \\ &= \sum_{n \in \mathcal{N}} \left[\frac{p_n D_n}{R_{k,z}^n} \right] + \sum_{k \in \mathcal{K}} \left[T_l C_k B_k \alpha f_k^2 + \frac{q_k d_k}{R_{fh}} \right]. \quad (12) \end{aligned}$$

III. PROBLEM FORMULATION

We propose to minimize the total energy consumption for a delay-constrained FL. Specifically, our proposed framework intelligently selects the active IoT devices that perform local learning and assigns active IoT devices to the suitable F-APs. Considering IoT device local learning scenario, the energy minimization problem can be formulated as

$$\begin{aligned} \mathcal{P}_1 : \quad & \min_{\mathbf{A}, \mathbf{S}, \mathbf{f}_N, \mathbf{p}} \sum_{n \in \mathcal{N}} \left[\frac{p_n d_n}{R_{k,z}^n} + T_l C_n D_n \alpha f_n^2 \right] \\ \text{s.t.} \quad & \left\{ \begin{array}{l} \text{C1: } \sum_{k \in \mathcal{K}} a_{k,n} = 1 \ \& \ \sum_{z \in \mathcal{Z}} s_{k,z}^n = 1, \forall n \in \mathcal{N}, \\ \text{C2: } \sum_{n \in \mathcal{N}} s_{k,z}^n \leq 2, \forall k \in \mathcal{K}, z \in \mathcal{Z}; \\ \text{C3: } f_n^{\min} \leq f_n \leq f_n^{\max}, \forall n \in \mathcal{N}, \\ \text{C4: } \tau_1 \leq T_q; \\ \text{C5: } 0 \leq p_n \leq p_{\max}, \forall n \in \mathcal{N}; \\ \text{C6: } a_{i,j} \in \{0, 1\}, s_{i,j}^k \in \{0, 1\}. \end{array} \right. \end{aligned}$$

In \mathcal{P}_1 , C1 indicates that each IoT device is scheduled to only one F-AP and to only one RRB in that F-AP; C2 indicates

that maximum two IoT devices can be scheduled to each F-AP at the same time; C3 is the constraint on local computation resource allocations of IoT devices; C4 indicates the QoS requirement on the FL time; and C5 is the transmit power control constraint.

The optimization problem of energy consumption minimization for FL integrated FCC-enabled IoT networks of the F-AP local learning scenario can be expressed as

$$\mathcal{P}_2 : \min_{\mathbf{A}, \mathbf{S}, \mathbf{I}_K, \mathbf{P}} \sum_{n \in \mathcal{N}} \left[\frac{p_n D_n}{R_{k,z}^n} \right] + \sum_{k \in \mathcal{K}} \left[T_l C_k B_k \alpha f_k^2 + \frac{q_k d_k}{R_{fh}} \right]$$

$$\text{s.t.} \begin{cases} \text{C1, C2, C5, C6,} \\ \text{C3: } f_k^{\min} \leq f_k \leq f_k^{\max}, \forall k \in \mathcal{K}, \\ \text{C4: } N_k \leq U, \forall k \in \mathcal{K}; \\ \text{C7: } \tau_2 \leq T_q. \end{cases}$$

In \mathcal{P}_2 , C3 is the constraint on local computation resource allocations of F-APs; C4 represents that the number of scheduled IoT devices to F-AP k N_k is less than or equal to the maximum number of scheduled IoT devices U . This is because each F-AP has certain computation frequency capability, and thus it can schedule only a limited number of IoT devices. Finally, C5 indicates the QoS requirement on the FL time. Note that both problems \mathcal{P}_1 and \mathcal{P}_2 are non-convex optimization problems. In addition, owing to the coupling of the optimization variables f_n , f_k and p_n , it is challenging to solve problems \mathcal{P}_1 and \mathcal{P}_2 . To this end, we divide both optimization problems into two subproblems and optimize them iteratively in order to achieve suboptimal yet practical solutions.

IV. ENERGY CONSUMPTION MINIMIZATION: FIRST SCENARIO

A. Problem \mathcal{P}_1 Transformation

Solving problem \mathcal{P}_1 owing to its mixed combinatorial characteristics is challenging. Although exhaustive search and branch-and-bound approaches can obtain near-optimal solution to \mathcal{P}_1 , such approaches are not suitable for the practical systems due to the significantly increased computational complexity. To strike a suitable balance between the required complexity and performance, we propose an iterative approach to solve problem \mathcal{P}_1 for large-scale IoT networks. To this end, we decompose \mathcal{P}_1 into the following two subproblems, namely, (i) IoT device scheduling and power allocation subproblem for a given IoT device' computation frequency allocation, and (ii) IoT device' computation frequency allocation subproblem for the determined power and IoT device scheduling.

IoT Device Scheduling and Power Allocation Subproblem: For a fixed set of computation frequency allocation, f_n^* , $\forall n \in \mathcal{N}$, the optimization problem \mathcal{P}_1 can be written as

$$\mathcal{P}_3 : \min_{\mathbf{A}, \mathbf{S}, \mathbf{P}} \sum_{n \in \mathcal{N}} \frac{p_n d_n}{W \log_2(1 + \gamma_{k,z}^n)}$$

$$\text{s.t.} \begin{cases} \text{C1, C2, C5,} \\ \text{C4: } T_l \frac{C_n D_n}{f_n} + \frac{d_n}{R_{k,z}^n} \leq T_{q,k}, \forall n \in \mathcal{N}, \end{cases}$$

where $T_{q,k} = T_q - \frac{\sum_{n \in \mathcal{N}_k} d_n}{R_{fh}}$. In \mathcal{P}_3 , the optimization is over the continuous variables \mathbf{p} , and the discrete variables $a_{k,n}$, and $s_{k,z}^n$, $\forall k \in \mathcal{K}, n \in \mathcal{N}, z \in \mathcal{Z}$. Nevertheless, it is still

challenging to solve problem \mathcal{P}_3 because of the non-convexity. We hence design an efficient yet low-complexity graph theory algorithm to tackle this problem in Section IV. B.

Computation Frequency Allocation Subproblem: For the given transmit power allocation and scheduling among the IoT devices, RRBs, and F-APs, problem \mathcal{P}_1 is reduced to the following subproblem

$$\mathcal{P}_4 : \min_{f_N} \sum_{n \in \mathcal{N}} T_l C_n D_n \alpha f_n^2$$

$$\text{s.t.} \begin{cases} \text{C3: } f_n^{\min} \leq f_n \leq f_n^{\max}, \forall n \in \mathcal{N}, \\ \text{C4: } \max_{n \in \mathcal{N}} \left\{ T_l \frac{C_n D_n}{f_n} + \frac{d_n}{R_{k,z}^n} \right\} \leq T_{q,k}. \end{cases}$$

C4 can be transformed into $T_l \frac{C_n D_n}{f_n} + \frac{d_n}{R_{k,z}^n} \leq T_{q,k}, \forall n \in \mathcal{N}$. Hence, the lower bound of IoT device's computation frequency can be calculated as $f_n \geq \frac{T_l C_n D_n}{T_{q,k} - \frac{d_n}{R_{k,z}^n}}$. For simplicity, we denote $\hat{f}_n = \frac{T_l C_n D_n}{T_{q,k} - \frac{d_n}{R_{k,z}^n}}$. Then, f_n satisfies $f_n \geq$

$\max \left\{ f_n^{\min}, \hat{f}_n \right\}$, and accordingly, C3 and C4 can be combined as $\max \left\{ f_n^{\min}, \hat{f}_n \right\} \leq f_n \leq f_n^{\max}$. Therefore, \mathcal{P}_4 can be expressed as

$$\mathcal{P}_5 : \min_{f_n} \sum_{n \in \mathcal{N}} T_l C_n D_n \alpha f_n^2$$

$$\text{s.t.} \max \left\{ f_n^{\min}, \hat{f}_n \right\} \leq f_n \leq f_n^{\max}, \forall n \in \mathcal{N}. \quad (17a)$$

Lemma 1: The closed-form solution of subproblem \mathcal{P}_5 is obtained as

$$f_n = \begin{cases} f_n^{\min}, & \text{if } \hat{f}_n \leq f_n^{\min} \\ \hat{f}_n, & \text{if } f_n^{\min} < \hat{f}_n < f_n^{\max} \\ f_n^{\max}, & \text{if } \hat{f}_n \geq f_n^{\max} \end{cases} \quad (18)$$

Proof. The proof is omitted due to the space limitation.

\mathcal{P}_1 is solved by iteratively solving both subproblems \mathcal{P}_3 and \mathcal{P}_5 until convergence. The overall algorithm to obtain a suitable solution to problem \mathcal{P}_1 is provided in Section IV-C.

B. Subproblem \mathcal{P}_3 Solution

In this subsection, we develop an effective and low complexity approach to solve the joint IoT device scheduling and power control subproblem \mathcal{P}_3 . Our developed solution designs a graph for all IoT device-RRB-F-AP feasible schedules and efficiently allocates power levels for the IoT devices in each schedule. The two-stage solution is explained as follows.

Stage 1: IoT Device Feasible Scheduling: In this stage, we design a graph that judiciously generates feasible NOMA clusters and jointly optimizes IoT devices-F-APs/RRBs assignments and transmit power of the IoT devices. This stage consists of graph design and maximum weight independent search (MWIS) method.

1) **Graph design:** Let $\mathcal{G} = (\mathcal{V}, \mathcal{E}, \mathcal{W})$ represents an undirected graph. The graph \mathcal{G} is constructed by generating a vertex v for each 2-IoT devices, RRB, and F-AP in the network as follows. We start from RRB $z = 1$, and assume that IoT device $n = 1$ is allocated to it. Then, we find the available NOMA clusters according to the possible two scenarios:

- 1) If IoT device $n = 1$ is not in the service area of the k -th F-AP, we check IoT device $n = 2$ for possible association

to RRB z and F-AP k , and then continue finding the second IoT device.

- 2) If IoT device $n = 1$ is in the service area of the k -th F-AP, then we find the second UD $j = n + 1$ (currently, $j = 2$), for the $(n = 1, z = 1)$ pair. Afterwards, we find p_n^*, p_j^* and calculate the rates, and then, we generate a vertex $v = \{(r_n^*, z, k), (r_j^*, z, k)\}$ that represents a feasible NOMA cluster. Given r_n^*, r_j^* , we then compute the weight of that vertex $w(v) = X_n + X_j$ and update \mathcal{G} . If adding $j = 2$ is infeasible, we let $j = j + 1 = 3$, and we verify the feasibility and repeat the aforementioned step.

In order to obtain all the feasible NOMA clusters $((n, j) \in \mathcal{N}, z \in \mathcal{Z}, k \in \mathcal{K}), j > n$, we iteratively repeat the above process (1), (2). The vertices in the designed graph \mathcal{G} that represent NOMA feasible clusters are connected by a conflict edge according to the following connectivity conditions (CCs):

- **CC1:** The same IoT devices (any IoT device or both IoT devices) are associated with both vertices v and v' .
- **CC2:** The same RRB in the same F-AP is associated with both vertices v and v' .

In summary, two distinct vertices v and v' representing two different NOMA clusters are connecting by a conflict edge if and only if the associations of RRBs and IoT devices (one or both associations) they represent are appeared in both vertices.

To select the IoT device-RRB-F-AP scheduling that provides a local minimum energy consumption, we design a proper weight $w(v)$ to each vertex $v \in \mathcal{G}$. For notation simplicity, we define the utility of IoT devices n and j as $X_n = T_l C_n D_n \alpha f_n^2 + \frac{p_n d_n}{R_{k,z}^n}$, $X_j = T_l C_j D_j \alpha f_j^2 + \frac{p_j d_j}{R_{k,z}^j}$, respectively. Therefore, the weight of vertex v that reflects the minimum energy consumption of IoT devices n, j can be given by

$$w(v) = X_{n^v} + X_{j^v}, \quad (19)$$

where X_{n^v} and X_{j^v} are the utility of associated IoT devices n and j to vertex v , respectively. The weight of vertex v in (19) is determined by the transmit powers $\{p_n^*, p_j^*\}$, computation frequency allocation $\{f_n^*, f_j^*\}$, RRB z^v , and F-AP k^v allocated to them.

2) **MWIS search method:** In this step, the algorithm iteratively and greedily selects the MWIS Γ^* among all the minimal independent sets Γ in the graph \mathcal{G} , where in each iteration we implement the following procedures. We compute the weight of all generated vertices using (19). The vertex with the minimum weight v^* is selected among all other corresponding vertices. The selected vertex v^* is, then, added to Γ^* that is initially empty. Afterwards, we update the \mathcal{G} graph by removing the selected vertices v^* and its connected vertices. As such, the next selected vertex is not in conflict connection with the already selected vertices in Γ^* . The process continues until no more vertices exist in \mathcal{G} . Since each RRB in each F-AP contributes by a single vertex, the number of vertices in Γ^* is ZK .

Stage 2: Power Allocation: From the designed \mathcal{G} , we obtain a set of vertices that represent NOMA clusters. Each NOMA cluster includes two IoT devices that simultaneously transmit to an F-AP over an RRB. For each vertex, we aim to determine transmit power allocations of the IoT devices such

that (i) the overall uplink transmission rate is improved by suppressing the interference between the IoT devices and (ii) the energy consumption for wireless transmission is reduced. Without loss of generality, we consider a vertex where the n -th and the j -th IoT devices are clustered, and both IoT devices transmit to the k -th F-AP over the z -th RRB. For such a vertex, we formulate the transmit power allocation subproblem as $\mathcal{P}_3 - 1$ at the top of the next page. In subproblem $\mathcal{P}_3 - 1$, $R_{th,n}$ and $R_{th,j}$ are the required uplink data rates for the n -th and j -th IoT devices, respectively; and V is a given weight factor. In particular, $R_{th,n} = \frac{T_g d_n}{T_{q,k} - T_g T_l \frac{C_n D_n}{f_n^*}}$ and

$$R_{th,j} = \frac{T_g d_j}{T_{q,k} - T_g T_l \frac{C_j D_j}{f_j^*}}. \text{ Essentially, the rate constraints C8}$$

and C9 satisfy the FL delay constraint C4. On the other hand, the weight factor V is selected to strike a suitable balance between capacity and energy consumption of the vertices.

Note that the power allocation depends on the channel gain of the associated IoT devices. To this end, we first define $\Delta_n = \frac{\sigma^2}{p_{\max}} (2^{R_{th,n}/W} - 1)$ and $\Delta_j = \frac{\sigma^2}{p_{\max}} (2^{R_{th,j}/W} - 1)$. Thereafter, we consider the following four cases: **Case I:** $|G_{k,z}^n|^2 < \Delta_n$ and $|G_{k,z}^j|^2 < \Delta_j$, **Case II:** $|G_{k,z}^n|^2 \geq \Delta_n$ and $|G_{k,z}^j|^2 < \Delta_j$, **Case III:** $|G_{k,z}^n|^2 < \Delta_n$ and $|G_{k,z}^j|^2 \geq \Delta_j$, and **Case IV:** $|G_{k,z}^n|^2 \geq \Delta_n$ and $|G_{k,z}^j|^2 \geq \Delta_j$. The transmit power allocations, (p_n^*, p_j^*) , for each case are given as follows

Case I: In this case, both IoT devices can not satisfy the rate constraints even using the maximum transmit power. Consequently, both IoT devices suspend their data transmission, and we obtain $p_n^* = 0$ and $p_j^* = 0$.

Case II: In this case, only the n -th IoT device can satisfy the required rate constraint, and the transmission of the j -th IoT device is suspended. Therefore, we obtain $p_j^* = 0$ and $p_n^* = \frac{\sigma^2}{|G_{k,z}^n|^2} (2^{R_{th,j}/W} - 1)$.

Case III: In this case, only the j -th IoT device can satisfy the required rate constraint, and the transmission of the n -th IoT device is suspended. Therefore, we obtain $p_n^* = 0$ and $p_j^* = \frac{\sigma^2}{|G_{k,z}^j|^2} (2^{R_{th,j}/W} - 1)$.

Case IV: In this case, both IoT devices can simultaneously transmit. Without loss of generality, we assume that $|G_{k,z}^j|^2 < |G_{k,z}^n|^2$, i.e., the n -th IoT device has a better channel gain compared to the j -th IoT device. According to the NOMA principle, the k -th F-AP first decodes the n -th IoT device's signal, and subsequently, decodes the j -th IoT device's signal after removing the interference from the n -th device via applying the SIC technique. We first introduce the following lemma to update the j -th IoT device's power allocation

Lemma 2: Assume that the given transmit power allocations for the n -th and the j -th IoT devices are \tilde{p}_n and \tilde{p}_j , respectively. Therefore, the j -th IoT device's transmit power allocation to maximize subproblem $\mathcal{P}_3 - 1$ is obtained as

$$p_j = \left[\frac{\frac{\gamma_{k,z}^j}{1 + \gamma_{k,z}^j}}{V + \frac{(\gamma_{k,z}^n)^2 |G_{k,z}^j|^2}{1 + \gamma_{k,z}^n \tilde{p}_n |G_{k,z}^n|^2}} \right]_{p_{th}}^{p_{\max}} \quad (20)$$

where $\gamma_{k,z}^n$ and $\gamma_{k,z}^j$ are calculated by plugging \tilde{p}_n and \tilde{p}_j

$$\begin{aligned} \mathcal{P}_3 - 1 : \quad & \max_{\substack{0 \leq p_n \leq p_{\max}, \\ 0 \leq p_j \leq p_{\max}}} W \left(\log_2(1 + \gamma_{k,z}^n) + \log_2(1 + \gamma_{k,z}^j) \right) - V(p_n + p_j) \\ \text{s.t.} \quad & \begin{cases} \text{C8: } W \log_2(1 + \gamma_{k,z}^n) \geq R_{th,n} \\ \text{C9: } W \log_2(1 + \gamma_{k,z}^j) \geq R_{th,j}. \end{cases} \end{aligned}$$

to (1), $p_{th} = \frac{\sigma^2}{|G_{k,z}^j|^2} (2^{R_{th,j}/W} - 1)$, and $[\cdot]_{p_{th}}^{p_{\max}}$ denotes projection in the range of $[p_{th}, p_{\max}]$.

Proof. The proof is omitted due to the space limitation.

We consider a suboptimal approach to iteratively update the transmit power allocation of both the n -th and the j -th IoT devices in inner and outer loop. Specifically, using a bi-section search method, the outer loop adjusts the power allocation of the n -th IoT device such that the rate constraint C8 is satisfied, and the inner loop adjusts the power allocation of the j -th IoT device according to Lemma 2. Let us denote the minimum and maximum power level for the n -th IoT device as $p_{n,low}$ and $p_{n,high}$. The initial transmit power of the n -th IoT device is obtained as $p_n = \frac{p_{n,low} + p_{n,high}}{2}$. By plugging the transmit power of the n -th IoT device to Lemma 2, the j -th IoT device's transmit power is determined. Thereafter, the achievable rate of the n -th IoT device is calculated. If $W \log_2(1 + \gamma_{k,z}^n) > R_{th,1}$, $p_{n,high} \leftarrow p_n$ is applied and if $W \log_2(1 + \gamma_{k,z}^n) < R_{th,1}$, $p_{n,low} \leftarrow p_n$ is applied. Then, the transmit power of the n -th IoT device is updated as $p_n = \frac{p_{n,low} + p_{n,high}}{2}$. The aforementioned procedures are repeated until $|W \log_2(1 + \gamma_{k,z}^n) - R_{th,1}|$ approaches a small value. The final values of p_n and p_j provide the required power allocations for the Case IV. The overall two-stage algorithm to the subproblem \mathcal{P}_3 is summarized in Algorithm 1.

C. Proposed Algorithm

Our proposed iterative scenario to the problem \mathcal{P}_1 is summarized in Algorithm 2. Line 4 initiates the computation frequency allocation. The loop in lines 5-9 alternatively obtains the solutions of subproblems \mathcal{P}_3 and \mathcal{P}_5 and terminates when $f_n^{(t)}$ does not change or the maximum number of iteration is reached. Specifically, line 6 calculates $p_n^{(t)}$ with fixed $f_n^{(t-1)}$ from the previous iteration and line 7 calculates $f_n^{(t)}$ with fixed $p_n^{(t)}$ from the current iteration.

D. Complexity Analysis

The computational complexity of Algorithm 2 is dominated by the required complexity of the graph construction stage of Algorithm 1. In order to generate all the vertices using the low-complexity graph punning method, a total of $\mathcal{O}(NKZ)$ computational complexity is required. The required complexity of connecting the generated vertices, i.e., the required complexity of finding neighborhood of the generated vertices is $\mathcal{O}((NKZ)^2)$. Therefore, the overall computational complexity of Algorithm 2 is obtained as $\mathcal{O}(NKZ + (NKZ)^2) \approx \mathcal{O}(N^2K^2Z^2)$.

V. ENERGY CONSUMPTION MINIMIZATION: SECOND SCENARIO

A. Problem \mathcal{P}_2 Transformation

We decompose \mathcal{P}_2 into two subproblems, namely, (i) joint power allocation and IoT device-F-AP/RRB scheduling optimization subproblem for fixed F-APs' computation frequency

Algorithm 1: Low Complexity Graph Algorithm

Data: $\mathcal{N}, \mathcal{K}, \mathcal{Z}, G_{k,z}^n, p_{\max}$, and f_n^* ,
 $(n, k, z) \in \mathcal{N} \times \mathcal{K} \times \mathcal{Z}$.

Stage 1: IoT device feasible scheduling

- Initialize $\mathcal{G} = \emptyset$.
- for** $k = 1 : K$ **do**
- for** $z = 1 : Z$ **do**
- Set $n = 1$
- if** the n -th IoT device in \mathcal{N}_k **then**
- Set $j = n + 1$
- while** $j < N$ **do**
- if** the j -th IoT device in \mathcal{N}_k **then**
- Based on p_n and p_j , calculate r_n, r_j
- Generate vertex
- $v = \{(r_n^*, z, k), (r_j^*, z, k)\}$ and set
- $\mathcal{G} \leftarrow \mathcal{G} \cup v$
- end if**
- $j = j + 1$
- end while**
- else**
- $n = n + 1$
- end if**
- end for**
- end for**

- For each $v \in \mathcal{V}$, finds its neighborhood $\mathcal{N}_{\mathcal{G}}(v)$ according to CC1 and CC2.
- Calculate the weight of each vertex $w(v)$ as in (19).
- Let $\Gamma^* = \emptyset, l = 0, \mathcal{G}_l = \mathcal{G}$.
- **MWIS Search Method:**
- while** $\mathcal{V}(\mathcal{G}_l) \neq \emptyset$ **do**
- $v^* = \arg \min_{v \in \mathcal{G}_l(\Gamma)} \{w(v)\}$ and set $\Gamma \leftarrow \Gamma \cup v^*$
- Let $\mathcal{V}(\mathcal{G}_{l+1}) = \mathcal{V}(\mathcal{G}_l(\Gamma))$
- $l = l + 1$
- end while**
- Output: The MWIS and its corresponding IoT device scheduling.

Stage 2: Power allocation: Allocate transmit power in the NOMA clusters according to the method described in Section IV-B.

allocation, and (ii) F-APs' computation frequency allocation that optimizes computation allocation.

IoT Device Scheduling and Power Allocation Subproblem: For a fixed set of F-APs' computation frequency allocation, $f_k^*, \forall k \in \mathcal{K}$, the optimization problem \mathcal{P}_2 can be written as

$$\mathcal{P}_6 : \min_{\mathbf{A}, \mathbf{S}, \mathbf{P}} \sum_{n \in \mathcal{N}} \frac{p_n D_n}{W \log_2(1 + \gamma_{k,z}^n)}$$

$$\text{s.t.} \quad \begin{cases} \text{C1, C2, C4, C5,} \\ \text{C7: } \max_{n \in \mathcal{N}_k} \left\{ \frac{D_n}{R_{k,z}^n} \right\} + T_l \frac{C_k B_k}{f_k^*} + \frac{d_k}{R_{fh}} \leq T_q, \forall k \in \mathcal{K}. \end{cases}$$

In \mathcal{P}_6 , the optimization is over the continuous variables \mathbf{p} , and

Algorithm 2: Proposed Iterative Algorithm

- 1: **Input:** $\mathcal{N}, \mathcal{K}, \mathcal{Z}, C_n D_n, T_l, W, \sigma^2, p_{\max}, T_q, f_n^{\min}$, and f_n^{\max} .
 - 2: **Output:** IoT device scheduling, p_n , and f_n .
 - 3: Initialize the number of iteration $t = 1, f_n^{(0)} = f_n^{\min}, f_n^{(1)} = f_n^{\max}, \forall n \in \mathcal{N}$.
 - 4: **while** $f_n^{(t)} \neq f_n^{(t-1)}$ and $t < T_{\max}$ **do**
 - 5: Solve \mathcal{P}_3 as in Algorithm 1.
 - 6: Calculate the solution $f_n^{(t)}$ of the problem \mathcal{P}_5 according to Lemma 1.
 - 7: $t = t + 1$.
 - 8: **end while**
 - 9: Return IoT device scheduling, $p_n^{(t)}$, and $f_n^{(t)}$.
-

the discrete variables $a_{k,n}$, and $s_{k,z}^n, \forall k \in \mathcal{K}, n \in \mathcal{N}, z \in \mathcal{Z}$. It is still difficult to solve problem \mathcal{P}_6 because of its non-convexity. To find a tractable solution to \mathcal{P}_6 , we develop an efficient algorithm in Section V-B.

Computation Frequency Allocation Subproblem: After obtaining $p_n, \forall n \in \mathcal{N}$ and IoT device-RRB-F-AP scheduling, problem \mathcal{P}_2 is reduced to

$$\mathcal{P}_7 : \min_{f_k} \sum_{k \in \mathcal{K}} \left[T_l C_k B_k \alpha f_k^2 + \frac{q_k d_k}{R_{fh}} \right]$$

$$\text{s.t.} \begin{cases} \text{C3: } f_k^{\min} \leq f_k \leq f_k^{\max}, \forall k \in \mathcal{K}, \\ \text{C7: } \max_{k \in \mathcal{K}} \left\{ \max_{n \in \mathcal{N}_k} \left\{ \frac{D_n}{R_{k,z}^n} \right\} + T_l \frac{C_k B_k}{f_k} + \frac{d_k}{R_{fh}} \right\} \leq T_q \end{cases}$$

Subproblem \mathcal{P}_7 can be equivalently expressed as

$$\mathcal{P}_8 : \min_{f_k} \sum_{k \in \mathcal{K}} \left[T_l C_k B_k \alpha f_k^2 + \frac{q_k d_k}{R_{fh}} \right]$$

$$\text{s.t.} \max \left\{ f_k^{\min}, \hat{f}_k \right\} \leq f_k \leq f_k^{\max}, \forall k \in \mathcal{K}, \quad (23a)$$

$$\text{where } \hat{f}_k = \frac{T_l C_k B_k}{T_q - \max_{n \in \mathcal{N}_k} \left(\frac{D_n}{R_{k,z}^n} \right) - \frac{d_k}{R_{fh}}}.$$

Lemma 3: The closed-form solution to \mathcal{P}_8 is obtained as

$$f_k = \begin{cases} f_k^{\min}, & \text{if } \hat{f}_k \leq f_k^{\min} \\ \hat{f}_k, & \text{if } f_k^{\min} < \hat{f}_k < f_k^{\max} \\ f_k^{\max}, & \text{if } \hat{f}_k \geq f_k^{\max} \end{cases} \quad (24)$$

Proof. The proof is omitted due to the space limitation.

B. Subproblem \mathcal{P}_6 Solution

This subsection first addresses the optimization subproblem \mathcal{P}_6 as an IoT device coordinated scheduling problem only, and can be written as

$$\mathcal{P}_9 : \min_{\mathbf{A}, \mathbf{S}} \sum_{n \in \mathcal{N}} \frac{p_n^* D_n}{W \log_2(1 + \gamma_{k,z}^n)}$$

$$\text{s.t.} \begin{cases} \text{C1: } \sum_{k \in \mathcal{K}} a_{k,n} = 1 \ \& \ \sum_{z \in \mathcal{Z}} s_{k,z}^n = 1, \forall n \in \mathcal{N}, \\ \text{C2: } \sum_{n \in \mathcal{N}} s_{k,z}^n \leq 2, \forall k \in \mathcal{K}, z \in \mathcal{Z} \\ \text{C4: } N_k \leq U, \forall k \in \mathcal{K}, \\ \text{C7: } \max_{n \in \mathcal{N}_k} \left\{ \frac{D_n}{R_{k,z}^n} \right\} \leq T_{q,k}, \forall n \in \mathcal{N}, \end{cases}$$

where $T_{q,k} = T_q - \left(T_l \frac{C_k B_k}{f_k^*} + \frac{d_k}{R_{fh}} \right)$. The optimization is carried over the variables \mathbf{A}, \mathbf{S} .

On the other hand, for the resulting IoT device-RRB/F-AP schedule, \mathcal{P}_6 can be considered as a power allocation step and simplifies per RRB basis. For each RRB z , the optimization problem \mathcal{P}_6 can be written as

$$\mathcal{P}_{10} : \min_{\mathbf{p}} \sum_{n \in \mathcal{N}} \frac{p_n D_n}{W \log_2(1 + \gamma_{k,z}^n)}$$

$$\text{s.t.} \begin{cases} \text{C5: } 0 \leq p_n \leq p_{\max}, \forall n \in \mathcal{N}, \\ \text{C7: } \max_{n \in \mathcal{N}_k} \left\{ \frac{D_n}{R_{k,z}^n} \right\} \leq T_{q,k}, \forall n \in \mathcal{N}, \end{cases}$$

where the optimization is over the set of powers $p_n, \forall n \in \mathcal{N}$. Note that solving the power allocation problem \mathcal{P}_{10} for the resulting IoT device-RRB/F-AP schedule is omitted in this section because it can follow the solution of $\mathcal{P}_3 - 1$ in Section IV-B.

The graph-based solution of the IoT coordinated scheduling problem \mathcal{P}_9 is explained as follows.

1) IoT Device Coordinated Scheduling: The NOMA-coordinated graph is introduced to jointly consider NOMA cluster per RRB, maximum number of IoT devices scheduled to F-AP, and transmission conflict. The NOMA-coordinated graph, denoted by $\mathcal{G}_{\text{NOMA}}(\mathcal{V}, \mathcal{E})$, is designed by generating all vertices for the k -th F-AP. The vertex set \mathcal{V} of the entire graph is the union of vertices of all F-APs. Consider, for now, generating the vertices of F-AP k . Therefore, each vertex $v_{k,z,n,j}$ is generated for each $z \in \mathcal{Z}$ and for every 2-IoT devices (n, j) in the service area of F-AP k . Similarly, we generate all vertices for all F-APs in \mathcal{K} . The configuration of the set of edges in the NOMA-coordinated graph is divided into IoT devices' association and transmission conflict edges. Two vertices $v_{k,z,n,j}$ and $v_{k',z',n',j'}$ representing different RRB z and the same F-AP k are adjacent by a conflict link if the number of scheduled IoT devices N_k to F-AP k is more than U . Similarly, two vertices $v_{k,z,n,j}$ and $v_{k',z',n',j'}$ are adjacent by a transmission conflict link if one of these conditions is true:

- $n = n'$ and/or $j = j'$. This condition schedules different IoT devices to different RRBs/F-APs.
- $z = z'$ and $k = k'$. This condition insists that same RRB in the same F-AP is associated with both vertices $v_{k,z,n,j}$ and $v_{k',z',n',j'}$.

Therefore, two vertices $v_{k,z,n,j}$ and $v_{k',z',n',j'}$ are adjacent by a conflict edge in \mathcal{E} if they satisfy one of the following CCs.

- **CC1:** $(n \neq n' \text{ and } j \neq j')$ and $(k = k' \text{ and } z \neq z')$, we have $N_k > U$.
- **CC2:** $n = n'$ and/or $j = j'$.
- **CC3:** $z = z'$ and $k = k'$.

Consider the weight of each vertex $v_{k,z,n,j}$ is defined as $w(v) = T_l C_k D_n \alpha f_k^2 + \frac{p_n D_n}{R_{k,z}^n} + T_l C_k D_j \alpha f_k^2 + \frac{p_j D_j}{R_{k,z}^n}$. Thus, the vertex' weight becomes small when the data transmission time from the represented IoT devices is small as well as the local computation time at the represented F-AP is small. This yields to a smart scheduling of IoT devices representing the corresponding vertex with a smaller weight, which in turn minimizes the energy consumption. Therefore, any minimal independent set in NOMA-coordinated graph represents a set of NOMA clusters that satisfies the following criterion: 1) each IoT device in the set is scheduled to only one F-AP

and one RRB, 2) each RRB identified by the vertices in a minimal independent set represents a NOMA cluster of two IoT devices, and 3) the total number of scheduled IoT devices at each F-AP is not larger than U .

The following theorem characterizes the solution of allocating IoT devices to the RRBs across all F-APs such that the total energy consumption is minimized.

Theorem 1: *The IoT device coordinated scheduling problem \mathcal{P}_9 is equivalent to MWIS problem over the NOMA-coordinated graph, wherein the weight of a vertex $v_{k,z,n,j}$ is given by*

$$w(v) = \alpha f_k^2 T_l C_k (D_n + D_j) + \frac{p_n D_n}{R_{k,z}^n} + \frac{p_j D_j}{R_{k,z}^j}. \quad (27)$$

The set of scheduled IoT devices to the z -th RRB in the k -th F-AP is obtained by combining the vertices of the MWIS \mathbf{I} in the NOMA-coordinated graph.

Proof. This theorem can be proved by demonstrating the following facts. The first fact establishes the equivalency between \mathcal{P}_9 and MWIS problems. Specifically, using $\mathcal{G}_{\text{NOMA}}$, \mathcal{P}_9 is similar to MWIS problems. In MWIS problems, two vertices must be nonadjacent in the graph, and similarly, in problem \mathcal{P}_9 , two NOMA clusters cannot be allocated with the same RRB or contain at least one IoT device. Afterward, the weight of each vertex is set to be the minimum energy consumption contribution of the corresponding NOMA cluster to the network. Therefore, the MWIS is a feasible solution with the minimum energy consumption, i.e., the MWIS is the feasible solution to \mathcal{P}_9 . To finalize the proof, we now prove that the weight of the MWIS is the objective function in \mathcal{P}_9 to be minimized. Let $\mathbf{I} = \{v_1, v_2, \dots, v_{|\mathbf{I}|}\}$, $v \in \mathcal{G}_{\text{NOMA}}$. Let a vertex $v \in \mathcal{V}$ is associated with 2-IoT devices NOMA cluster (n, j) . The weight of the MWIS over all the vertices that are representing the corresponding NOMA clusters over all RRBs/F-APs can be written as

$$\begin{aligned} w(\mathbf{I}) &= \sum_{v \in \mathbf{I}} w(v) \\ &= \sum_{k \in \mathcal{K}} \sum_{z \in \mathcal{Z}} \left(\alpha f_k^2 T_l C_k (D_n + D_j) + \frac{p_n D_n}{R_{k,z}^n} + \frac{p_j D_j}{R_{k,z}^j} \right). \end{aligned} \quad (28)$$

Therefore, the problem of minimizing the energy consumption \mathcal{P}_9 is equivalent to the MWIS problem among the minimal sets in the NOMA coordinated graph. \square

2) **Heuristic Solution:** MWIS problems are NP-hard problems, where the required complexity of solving these problems optimally requires an exhaustive search of $|\mathcal{V}|^2 \cdot 2^{|\mathcal{V}|}$ complexity where \mathcal{V} is the set of vertices of graph $\mathcal{G}_{\text{NOMA}}$. However, MWIS problems can be heuristically solved with a reduced complexity of $b^{|\mathcal{V}|}$ where b is the complexity constant [36], [37]. Thus, the MWIS problem can be solved effectively using a low-complexity heuristic solution.

Let $w(v)$ be the raw weight of vertex v in the NOMA coordinated graph as expressed in (27). The modified weight $\tilde{w}(v)$ of vertex v can be defined as

$$\tilde{w}(v) = w(v) \sum_{v' \in \mathcal{V}_v} w(v'), \quad (29)$$

Algorithm 3: Coordinated Scheduling Algorithm

Data: $\mathcal{N}, \mathcal{K}, \mathcal{Z}, p_{\max}, f_k^{\min}, f_k^{\max}, T_q, C_k D_k, d_k$, and $\mathcal{G}_{k,z}^n, (n, k, z) \in \mathcal{N} \times \mathcal{K} \times \mathcal{Z}$.

Phase I: IoT device coordinated scheduling

- Initialize $\mathcal{G}_{\text{NOMA}} = \emptyset, \mathbf{I} = \emptyset$.
- Construct $\mathcal{G}_{\text{NOMA}}$ using Section V-B.
- For each $v \in \mathcal{G}_{\text{NOMA}}$, calculate $w(v)$ and $\tilde{w}(v)$ using (27), (29), respectively
- Solve the MWIS problem in $\mathcal{G}_{\text{NOMA}}$ to find \mathbf{I} as follows:

while $\mathcal{G} \neq \emptyset$ **do**

$v^* = \min_{v \in \mathcal{G}_{\text{NOMA}}} \{w(v)\}$

Set $\mathbf{I} = \mathbf{I} \cup v^*$ and set $\mathcal{G}_{\text{NOMA}} = \mathcal{G}_{\text{NOMA}}(v^*)$

Continue only with vertices not linked to v^* in $\mathcal{G}_{\text{NOMA}}$

end while
- Output: The MWIS \mathbf{I} .
- For the resulting \mathbf{I} , solve the power allocation problem \mathcal{P}_{10} .
- Continue iterating between finding \mathbf{I} and solving \mathcal{P}_{10} until convergence.

Phase II: F-APs' computation frequency allocation

- Solve \mathcal{P}_8 for the resulting \mathbf{I} and power allocation.

for $v = \{v_1, v_2, \dots, |\mathbf{I}|\}$ **do**

Calculate $\hat{f}_k = \frac{T_l C_k B_k}{T_q - \max_{n \in \mathcal{N}_k} \left(\frac{D_n}{R_{k,z}^n} \right) - \frac{d_k}{R_{f_h}}}$,

$\forall (k, z, n)$ is associated with v

Calculate f_k according to Lemma 3

end for
 - Execute phases 1 and II until convergence or a maximum number of iteration is reached.
 - Obtain \mathbf{I} and \mathbf{f}_K .
-

where \mathcal{V}_v is the set of vertices not connected to vertex v by transmission conflict edges. The appropriate design of the weights shows that \tilde{w}_v reflects the contribution of the vertex to the network as it has a small raw weight and non-adjacent to a large number of vertices induced by users with small raw weight. The two-phase scenario of IoT device coordinated scheduling and F-AP's computation frequency allocation is presented in Algorithm 3.

C. Complexity Analysis

The computational complexity of Algorithm 3 is dominated by the required complexity of generating feasible NOMA clusters and connecting the generated vertices. To generate all the vertices using the low-complexity graph method, a total of $\mathcal{O}\left(KZ \binom{|\mathcal{N}_k|}{2}\right)$ computational complexity is required. On the other hand, the required complexity of connecting the generating vertices, i.e., the required complexity of finding neighborhood of the generated vertices is $\mathcal{O}\left(\left(KZ \binom{|\mathcal{N}_k|}{2}\right)^2\right)$. Therefore, the overall computational complexity of Algorithm 3 is obtained as $\mathcal{O}\left(NKZ + \left(KZ \binom{|\mathcal{N}_k|}{2}\right)^2\right) \approx \mathcal{O}\left(\left(KZ \binom{|\mathcal{N}_k|}{2}\right)^2\right)$.

TABLE I: Simulation Parameters

Parameter	Value
Circle radius of F-AP's service area R	500 m
learning local parameter size, d_n, d_k	[5 – 10] Kbit [21]
IoT device data size, D_n	[0.5 – 1] Mbit
IoT device processing density, C_n	[600 – 800] [21]
F-AP processing density, C_k	[1000 – 1500]
IoT device computation frequency, f_n	[0.0003 – 1] G cycles/s [21]
F-AP computation frequency, f_k	[0.0005 – 5] G cycles/s
CPU architecture based parameter, α	10^{-28} [33]

VI. NUMERICAL RESULTS

A. Simulation Setting and Schemes Under Consideration

In our simulations, we consider a hexagonal cell of radius 1500 m where F-APs and CS have fixed locations and IoT devices are distributed randomly within the cell. The CS is located at the cell center. The channel model for IoT device-F-AP transmissions follows the standard path-loss model, which consists of three components: 1) path-loss of $128.1 + 37.6 \log_{10}(\text{dis.}[\text{km}])$; 2) log-normal shadowing with 4 dB standard deviation; and 3) Rayleigh channel fading with zero-mean and unit variance. The noise power, F-AP's power, and maximum IoT device power are assumed to be -174 dBm/Hz and $q_k = p_{\max} = 3$ W, respectively [25]. The weighting factor V is set to 0.3. The total number of global and local FL iterations are calculated as $T_g = \frac{2\beta^2}{(2\vartheta - \beta\eta)\vartheta\eta} \ln(1/\epsilon_g)$, $T_l = \frac{2}{(2 - \delta\beta)\delta\vartheta} \ln(1/\epsilon_l)$, respectively, with $\beta = 4, \eta = 1/3, \delta = 1/4, \vartheta = 2, \epsilon_g = \epsilon_l = 10^{-3}$ [21]. The FL time threshold T_q is 1 second [21]. The bandwidth of each RRB is 20 MHz. Unless otherwise stated, we set the numbers of F-APs and RRBs to 9 and 4, respectively. The fronthaul capacity R_{fh} is set to 150 Mbit/s. For each IoT device and each F-AP, the number of data samples D_n is randomly chosen from 800 to 1000. Other parameters are summarized in Table I. To assess the performance of our proposed scenarios, we simulate various scenarios with different number of IoT devices N , data size D_n , number of RRBs Z , number of data samples D_n , computation frequency allocation f_n, f_k , and parameter data size. For the sake of comparison, our proposed schemes are compared with the following baseline schemes.

- **Power-only:** This scheme minimizes the energy consumption by optimizing the power level of IoT devices and fixing the computation frequency allocation to its maximum value.
- **Computation frequency-only:** This scheme, denoted by *CPU-only*, minimizes the energy consumption by optimizing the computation frequency allocation and fixing the power level to its maximum value.
- **Fixed:** This scheme employs random IoT device scheduling and fixes both the computation frequency allocation and transmission power to their maximum values.

B. Simulation Results and Discussions

We adopt two performance metrics as follows: (i) the *energy consumption* that represents the objective in \mathcal{P}_1 for the IoT device local learning scenario and \mathcal{P}_2 for the F-AP local learning scenario, and (ii) the *FL time* as expressed in (3).

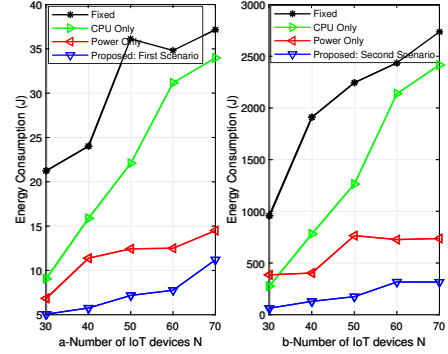


Fig. 3: Energy consumption vs. number of IoT devices N for $K = 9$ and $Z = 4$.

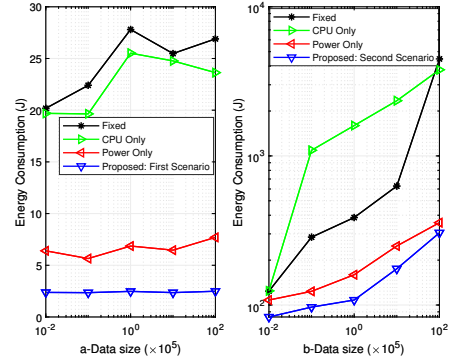


Fig. 4: Energy consumption vs. data size for $N = 50, K = 9$ and $Z = 4$.

1) *Consumption energy performance:* In Figs. 3-a and 3-b, we plot the energy consumption versus the number of IoT devices for the first and second scenarios, respectively. Our proposed schemes have the following two attributes. First, they judiciously schedule IoT devices to F-APs/RRBs, adapt the transmission rate of each IoT device, and optimize the transmission power of each IoT device. Second, our proposed schemes efficiently optimize the computation frequency allocation of IoT devices and F-APs. Leveraging these two attributes, our proposed schemes significantly reduce the energy consumption compared to the benchmark schemes, as depicted from both Figs. 3-a and 3-b. In particular, the *power-only* scheme selects the maximum computation frequency allocation for each IoT device and each F-AP. Consequently, the *power-only* scheme results in higher energy consumption for local learning, and it increases the energy consumption of the system in both scenarios. The *CPU-only* scheme ignores the power optimization that leads to more interference among the IoT devices and increased offloading transmission time. As a result, the *CPU-only* scheme leads to a high energy consumption. Finally, the *fixed* scheme has the most energy consumption because it chooses the maximum CPU frequency and transmission power. Accordingly, from an energy consumption perspective, it is inefficient to offload data to F-APs while ignoring the power allocation and employing random IoT device scheduling to F-APs/RRBs.

In Figs. 4-a and 4-b, we plot the energy consumption versus the data size D_n for the first and second scenarios,

respectively. When the data size is small (around 1 Kbit), both proposed schemes work superior in terms of minimizing the energy consumption. When the data size is nearly 10 Mbit, the energy consumption performance of our proposed first scheme does not change much and has a performance of 3 J. This is because the IoT devices perform local learning on the data and offload the local learning parameters only. However, when the data size changes from 1 Kbit to 10 Mbit, the energy consumption performance of the proposed second scheme changes from 1 J to around 303 J. Therefore, our proposed second scheme consumes more energy when the data size increases. Accordingly, from an energy consumption perspective, learning at the IoT devices as in the first proposed scenario is more efficient, especially for large numbers of IoT devices and large data sizes.

In Figs. 5-a and 5-b, we show the energy consumption versus the number of data samples D_n for the first and second scenarios, respectively. The number of data samples affects the CPU-related energy consumption. Similar to our discussions for Fig. 3, the *CPU-only* and *fixed* schemes severely degrade the energy consumption performance. Specifically, the energy consumption of the *fixed* scheme is increased with the number of data samples. However, the energy consumption of the *power-only* and our proposed schemes do not significantly change, e.g., see Fig. 5-(a). Since the energy consumption in the second scenario is dominated by data offloading to F-APs, both *CPU-only* and *fixed* schemes consume high energy as can be seen from Fig. 5-(b). Using the optimized resource allocations, our proposed schemes incur the least energy consumption for both small and large data samples.

In Figs. 6-a and 6-b, we plot the energy consumption versus the number of RRBs Z for the first and second scenarios, respectively. As can be seen, the consumed energy of all schemes are increased with the increase in the number of RRBs. This is due to the fact that as the number of RRBs increases, more IoT devices are scheduled, which in turn increases the energy consumption. Specifically, when $Z = 1$, the maximum number of accommodated IoT devices by the F-APs is $2ZK = 2 \times 1 \times 9 = 18$, thus the consumed energy of all schemes is low. As the number of RRBs is increased, the energy consumption of all the schemes is increased. This can be explained by the fact that when the number of RRBs goes beyond 2, no more IoT devices can be accommodated. Thus, the consumed energy of all schemes do not change much. For a fair comparison, we consider that all the schemes serve the same set of IoT devices in the available RRBs of a given F-AP. The proposed schemes, however, benefit from optimizing the transmit power and computation frequency allocation. Essentially, the proposed schemes achieve reduced energy consumption compared to the benchmark schemes.

In Figs. 7-a and 7-b, we show the energy consumption versus the number of CPU cycles for the first and second scenarios, respectively. The number of CPU cycles ranges from 2×10^7 to 10×10^7 in Fig. 7-(a) and from 2×10^9 to 10×10^9 in Fig. 7-(b). The number of CPU cycles determines the energy consumption. Hence, the energy consumption of both *fixed* and *power-only* schemes, that fix the computation frequency allocation at the highest value, is considerably

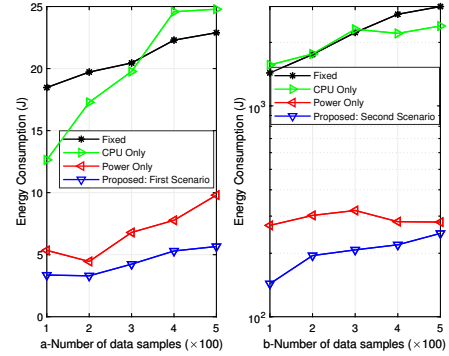


Fig. 5: Energy consumption vs. number of data samples for $N = 50$, $K = 9$ and $Z = 4$.

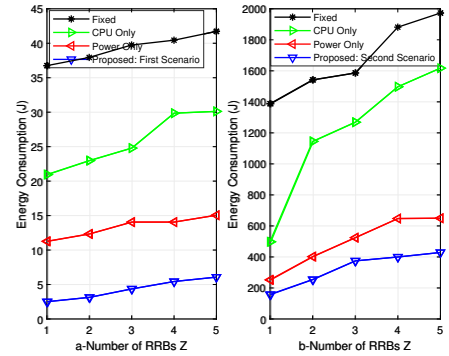


Fig. 6: Energy consumption vs. number of RRBs Z for $N = 50$ and $K = 9$.

increased with the increasing number of computation cycles. On the other hand, the energy consumption of both *CPU-only* and proposed schemes with adjustable CPU frequencies do not change much as shown in Figs. 7-a and 7-b. As expected, using both transmit power and computation frequency allocation, our proposed schemes incur the least energy consumption for both small and large numbers of CPU cycles.

2) *FL time performance*: In Fig. 8, Fig. 9, and Fig. 10, we plot the federated learning time versus: (a) number of IoT devices N , (b) number of data samples D_n , and (c) parameter data size d_n , respectively. First, it is clear that the FL time depends on the transmission time and the computation learning time of IoT devices. Since the local learning parameters have small size, the transmission time for offloading such parameters to F-APs/CS requires smaller portion of the overall FL time compared with the computation training time. Consequently, the FL time is dominated by the computation training time. As can be seen from Figs. 8, 9, 10, *fixed* scheme, that chooses the maximum CPU frequency, effectively minimizes the FL time at the cost of consuming the most energy as shown in Fig. 3 to Fig. 7. Our proposed first scheme that considers IoT device local learning, denoted by *proposed*, adjusts the CPU frequency and power transmissions so that it effectively minimizes the consumed energy within the FL time of 1 second. In Figs. 8, 10, the FL time of all algorithms does not change much with the number of IoT devices and local parameter size. This is because the FL time is mainly controlled by the longest local training time of one IoT device,

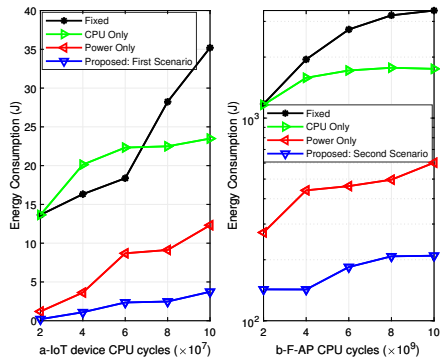


Fig. 7: Energy consumption vs. computation frequency for $N = 50$, $K = 9$ and $Z = 4$.

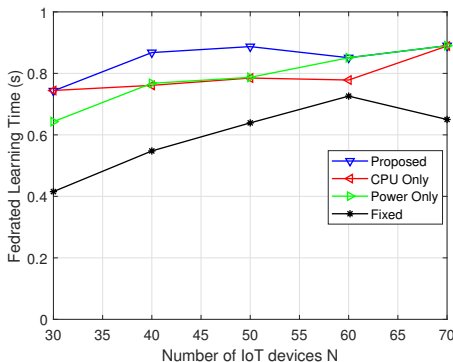


Fig. 8: Federated learning time vs. number of IoT devices N for $K = 9$ and $Z = 4$.

which does not significantly change when the number of IoT device and the local parameter size are increased.

Finally, we provide some observations from our presented simulation results as follows. First, although the *fixed* scheme performs fairly well in terms of reducing the FL time, it exhibits a poor energy consumption performance, which is impractical. Thus, it only serves as a benchmark scheme in this work. Second, it is advantageous to optimize the computation frequency allocation of the IoT devices and the F-APs as in the *CPU-only* scheme. However, it is inefficient to ignore the power optimization that significantly impacts the energy consumption of the system. Third, the *power-only* scheme works well in terms of reducing the energy consumption; however, its performance is degraded since it uses the maximum CPU of each IoT and each F-AP. Fourth, our proposed schemes strike a balance between the aforementioned aspects by judiciously scheduling IoT devices to F-APs/RRBs, adapting the transmission rate of each IoT device, and optimizing the transmission power of each IoT device. Furthermore, our proposed schemes efficiently optimize the computation frequency allocation of IoT devices and F-APs. Finally, as the data size increases, the energy consumption performance of the second proposed scheme degrades. This is because as the data size increases, the transmission time for offloading IoT devices' data to F-APs is significantly increased. Thus, the energy efficiency of our proposed first scheme becomes more pronounced compared to our second proposed scheme.

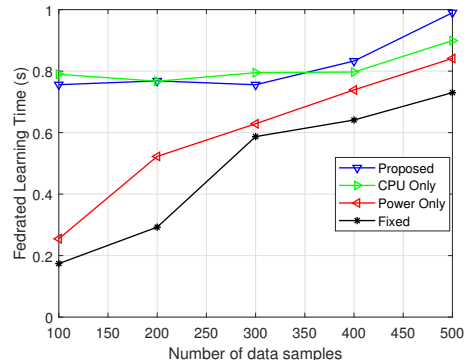


Fig. 9: Federated learning time vs. number of data samples D_n for $K = 9$ and $Z = 4$.

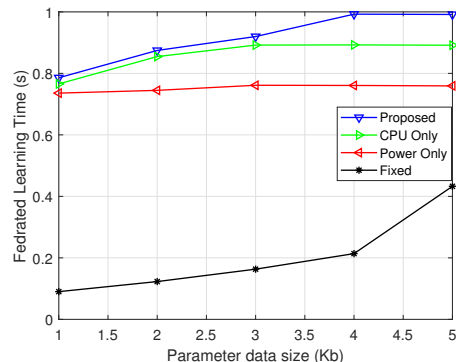


Fig. 10: Federated learning time vs. parameter data size d_n for $K = 9$ and $Z = 4$.

VII. CONCLUSION

In this paper, we investigated the resource allocation strategy to minimize the energy consumption for performing FL in an integrated FCC-enabled IoT network subject to FL time constraint. Specifically, we considered two scenarios for training the local models, and for both scenarios, we proposed joint optimization of computation frequency allocation, IoT device scheduling, and transmission power control of network edge devices. Leveraging graph theory, we proposed efficient iterative schemes. The presented numerical results revealed that the proposed schemes substantially reduce the energy consumption compared to the baseline solutions, at the cost of small increase of FL learning time. The presented simulation results interestingly revealed that for a large number of IoT devices and large data sizes, it is more energy efficient to train the local models at the IoT devices instead of the F-APs.

REFERENCES

- [1] T. K. Rodrigues *et al.* "Machine learning meets computation and communication control in evolving edge and cloud: Challenges and future perspective," *IEEE Commun. Surv. Tut.*, vol. 22, no. 1, pp. 38-67, Firstquarter 2020.
- [2] M. Mohammadi, A. Al-Fuqaha, S. Sorour, and M. Guizani, "Deep learning for IoT big data and streaming analytics: A survey," *IEEE Commun. Surv. Tut.*, vol. 20, no. 4, pp. 2923-2960, Oct.-Dec. 2018.
- [3] Y. Mao, C. You, J. Zhang, K. Huang, and K. B. Letaief, "A survey on mobile edge computing: The communication perspective," *IEEE Commun. Surv. Tut.*, vol. 19, no. 4, pp. 2322-2358, Fourthquarter 2017.

- [4] E. Baccarelli, P. G. V. Naranjo, M. Scarpiniti, M. Shojafar, and J. Abawajy, "Fog of everything: Energy-efficient networked computing architectures, research challenges, and a case study," *IEEE Access*, vol. 5, pp. 9882-9910, May 2017.
- [5] M. S. Al-Abiad, M. J. Hossain, and S. Sorour, "Cross-layer cloud offloading with quality of service guarantees in Fog-RANs," in *IEEE Trans. on Commun.*, vol. 67, no. 12, pp. 8435-8449, Jun. 2019.
- [6] M. S. Al-Abiad and M. J. Hossain, "Completion time minimization in Fog-RANs using D2D communications and rate-aware network coding," in *IEEE Trans. on Wireless Commun.*, vol. 20, no. 6, pp. 3831-3846, Jun. 2021.
- [7] M. Z. Hassan *et al.*, "Energy-spectrum efficient content distribution in fog-RAN using rate-splitting, common message decoding, and 3D-resource matching," *IEEE Trans. on Wireless Commun.*, Early Access, Mar. 2021.
- [8] M. Z. Hassan *et al.* "Joint throughput-power optimization of Fog-RAN using rate-splitting multiple access and reinforcement-learning based user clustering," *IEEE Trans. Veh. Technol.*, Early Access, Jun. 2021.
- [9] Y. Liu *et al.*, "Distributed resource allocation and computation offloading in fog and cloud networks with non-orthogonal multiple access," *IEEE Trans. Veh. Technol.*, vol. 67, no. 12, pp. 12 137-12 151, Dec. 2018.
- [10] Z. Yang, M. Chen, K. K. Wong, H. V. Poor, and S. Cui, "Federated learning for 6G: Applications, challenges, and opportunities," [Online]. Available: <https://arxiv.org/pdf/2101.01338>.
- [11] K. Bonawitz *et al.*, "Towards federated learning at scale: System design," *Proc. System Machine Learning Conf.*, Stanford, CA, USA, Feb. 2019.
- [12] S. Niknam, H. S. Dhillon, and J. H. Reed, "Federated learning for wireless communications: Motivation, opportunities, and challenges," *IEEE Commun. Mag.*, vol. 58, no. 6, pp. 46-51, Jun. 2020.
- [13] Z. Zhao, C. Feng, H. H. Yang, and X. Luo, "Federated-learning-enabled intelligent fog radio access networks: Fundamental theory, key techniques, and future trends," *IEEE Wireless Commun.*, vol. 27, no. 2, pp. 22-28, Apr. 2020.
- [14] M. Chen *et al.*, "Distributed learning in wireless networks: Recent progress and future challenges," [Online]. Available: <https://arxiv.org/pdf/2104.02151>.
- [15] H. B. McMahan, E. Moore, D. Ramage, S. Hampson, and B. A. Arcas, "Communication-efficient learning of deep networks from decentralized data," in *Proc. 20th Int. Conf. Artif. Intell. Stat. (AISTATS)*, pp. 1273-1282, Apr. 2017.
- [16] C. B. Issaid *et al.*, "Communication efficient distributed learning with censored, quantized, and generalized group ADMM," [Online]. Available: <https://arxiv.org/pdf/2009.06459>.
- [17] M. Chen, H. V. Poor, W. Saad, and S. Cui, "Wireless communications for collaborative federated learning," [Online]. Available: <https://arxiv.org/pdf/2006.02499>.
- [18] M. M. Wadu, S. Samarakoon, and M. Bennis, "Joint client scheduling and resource allocation under channel uncertainty in federated learning," *IEEE Trans. Commun.*, Early Access, Jun. 2021.
- [19] M. S. H. Abad *et al.*, "Hierarchical federated learning across heterogeneous cellular networks," [Online]. Available: <https://arxiv.org/pdf/1909.02362>.
- [20] M. Chen *et al.*, "A joint learning and communications framework for federated learning over wireless networks," *IEEE Trans. on Wireless Commun.* vol. 20, no. 1, pp. 269-283, Jan. 2021.
- [21] J. Yao and N. Ansari, "Secure federated learning by power control for internet of drones," *IEEE Trans. on Cognitive Commun. and Netw.*, Early Access, Apr. 2021.
- [22] Q. Zeng, Y. Du, K. K. Leung, and K. Huang, "Energy-efficient radio resource allocation for federated edge learning," [Online]. Available: <http://arxiv.org/abs/1907.06040>.
- [23] S. Wang *et al.*, "Adaptive federated learning in resource constrained edge computing systems," *IEEE J. Sel. Areas Commun.*, vol. 37, no. 6, pp. 1205-1221, Jun. 2019.
- [24] Z. Yang *et al.*, "Energy efficient federated learning over wireless communication networks," *IEEE Trans. on Wireless Commun.*, vol. 20, no. 3, pp. 1935-1949, Mar. 2021.
- [25] J. Yao and N. Ansari, "Enhancing federated learning in fog-aided IoT by CPU frequency and wireless power control," in *IEEE Int. of Things Journal*, vol. 8, no. 5, pp. 3438-3445, Mar. 2021.
- [26] H. Tran, G. Kaddoum, H. Elgala, C. Abou-Rjeily, and H. Kaushal, "Lightwave power transfer for federated learning-based wireless networks," *IEEE Commun. Lett.*, vol. 24, no. 7, pp. 1472-1476, Jul. 2020.
- [27] Y. Sarikaya and O. Ercetin, "Motivating workers in federated learning: A Stackelberg game perspective," *IEEE Netw. Lett.*, vol. 2, no. 1, pp. 23-27, Mar. 2020.
- [28] Z. Ding, J. Xu, O. A. Dobre, and H. V. Poor, "Joint power and time allocation for NOMA-MEC offloading," *IEEE Trans. Veh. Technol.*, vol. 68, no. 6, pp. 6207-6211, Jun. 2019.
- [29] M. S. Al-Abiad, M. Z. Hassan, A. Douik, and M. J. Hossain, "Low-complexity power allocation for network-coded user scheduling in Fog-RANs," in *IEEE Commun. Letters*, vol. 25, no. 4, pp. 1318-1322, Apr. 2021.
- [30] M. S. Al-Abiad, A. Douik, S. Sorour, and Md. J. Hossain, "Throughput maximization in cloud-radio access networks using rate-aware network Coding," *IEEE Trans. Mobile Comput.*, Early Access, Aug. 2020.
- [31] A. P. Miettinen and J. K. Nurminen, "Energy efficiency of mobile clients in cloud computing," in *Proc. 2nd USENIX Conf. Hot Topics Cloud Comput. (HotCloud)*, Berkeley, CA, USA, 2010, p. 4.
- [32] Q. Mao, F. Hu, and Q. Hao, "Deep learning for intelligent wireless networks: A comprehensive survey," *IEEE Commun. Surveys Tuts.*, vol. 20, no. 4, pp. 2595-2621, Fourthquarter, 2018.
- [33] A. P. Chandrakasan, S. Sheng, and R.W. Brodersen, "Low-power CMOS digital design," *IEEE J. Solid-State Circuits*, vol. 27, no. 4, pp. 473-484, Apr. 1992.
- [34] T. D. Burd and R. W. Brodersen, "Processor design for portable systems," *J. VLSI Signal Process Syst. Signal Image Video Technol.*, vol. 13, no. 2, pp. 203-221, Aug. 1996.
- [35] A. Douik, H. Dahrouj, O. Amin, B. AlOquibi, T. Y. A.-Naffouri, and M.-S. Alouini, "Mode selection and power allocation in multi-level cache-enabled networks," *IEEE Commun. Lett.*, vol. 24, no. 8, pp. 1789-1793, Aug. 2020.
- [36] K. Yamaguchi and S. Masuda, "A new exact algorithm for the maximum weight clique problem," in *Proc. Of the 23rd International Technical Conference on Circuits/Systems, Computers and Commun. (ITCCSCC'08)*, Yamaguchi, Japan.
- [37] P. R. J. Ostergard, "A fast algorithm for the maximum clique problem," *Discrete Appl. Math.*, vol. 120, pp. 197-207.